Struct Multidisc Optim (2007) 33: 61–70
DOI 10.1007/s00158-006-0033-y

INDUSTRIAL APPLICATION

S. Pierret · R. Filomeno Coelho · H. Kato

Multidisciplinary and multiple operating points shape optimization of three-dimensional compressor blades

Received: 28 June 2005 / Revised manuscript received: 6 March 2006 / Published online: 16 August 2006

Abstract The recent progress in simulation technologies in several fields such as computational fluid dynamics, structures, thermal analysis, and unsteady flow combined with the emergence of improved optimization algorithms makes it now possible to develop and use automatic optimization software and methodologies to perform complex multidisciplinary shape optimization process. In the present applications, the MAX optimization software developed at CENAERO is used to perform the optimization. This software allows performing derivative free optimization with very few calls to the computer intensive simulation software. The method employed in this paper combines the use of a genetic algorithm (with real coding of the variables) to an approximate (or meta) model to accelerate significantly the optimization process. The performance of this optimization methodology is illustrated on the optimization of three-dimensional turbomachinery blades for multiple operating points and multidisciplinary objectives and constraints. The NASA rotor 67 geometry is used to demonstrate the capabilities of the method. The aim is to find the optimal shape for three different operating conditions: one at a near peak efficiency point, one at choked mass flow, and one near the stall flow. The three points are analyzed at the same blade rotational speed but with different mass flows. A finite element structural mechanics software is used to compute the static and dynamic mechanical responses of the blade. A Navier–Stokes solver is used to calculate the aerodynamic performance. High performance computers (HPC) are used in this application. Cenaero's HPC infrastructure contains a Linux cluster with 170 3.06 GHz Xeon processors. The optimization algorithm is parallelized using MPI.

Keywords Optimization · Turbomachines · Multiobjectives · Genetic algorithms · Approximate models

S. Pierret (✉) · R. Filomeno Coelho · H. Kato
CENAERO asbl, Avenue Jean Mermoz 30, Bâtiment Mermoz 1, 6041 Gosselies, Belgium
e-mail: stephane.pierret@cenaero.be

1 Introduction

The pressure towards increased efficiency and reduction of the development and manufacturing costs and time has always pushed engineers to develop better and faster design methods.

Traditionally, the three dimensional blade shape is very often designed by experienced designers able to iteratively and manually modify the blade shape taking into account several results coming from aerodynamic computations (CFD) and finite element (FEM) structural mechanics computations (static and dynamic). In recent years, large progress has been made in the development of automatic optimization packages able to optimize complex shape using advanced CFD solver and optimization algorithms. Although these optimization methodologies are starting to be used in industry, they are not yet used very intensively in the real multidisciplinary shape optimization design process. A more intensive use still requires progress in the field of automatic shape optimization. Some of these are listed below:

– The type of multidisciplinary simulation involved in this research requires between 1 and 10 h per function evaluation. In this type of optimization problem, the number of design variables that can be treated simultaneously by the automatic optimization chain must be increased from less than 10 (in most of the existing industrial applications) to more than 100 required by realistic industrial design problems. This first limitation can be avoided by the use of the optimization techniques based on a genetic algorithm largely accelerated by the use of an approximate model such as a radial basis function network. This algorithm has proved to be capable of handling a large number of design variables for shape optimization (Pierret 2005).
– The automatic design optimizations are very often performed at a single operating condition leading to nonrobust optimal solution with very narrow optimal operating range. Therefore, a realistic automatic optimization methodology must include optimization at several operating points. This requires increased simulation time, very robust analysis packages, and optimization methods capable of handling uncomputable functions. An uncomputable

function means that the simulation package (CFD or FEM software) cannot provide a converged solution for some combination of design variables. In this case, the optimization method must flag this geometry as uncomputable, a penalty is added to this design point and the optimizer will move further away from this uncomputable design points during the next optimization cycles. The uncomputable penalty is scaled using the maximum value of the objective function found in the database. The spatial extention of this penalty is based on the use of an external penalty term scaled with the distance between the uncomputable point and the closest computable point.

– The number of physics usually included in the automatic optimization is very often limited to only one (i.e., CFD); the other physics (i.e., mechanics) are usually treated as simple side constraints (minimum thickness, etc.) during the optimization. This methodology must be improved by increasing the number of physics (aero, mechanics both static and dynamic) directly included in the optimization process. As an example, this can be performed by the use of detailed FEM simulation software and/or multiphysics simulations instead of using very simple geometrical criteria to check the mechanical constraints.
– The shape parametrization plays a very important role in the performance of the shape optimization process. A review of existing methods is presented in (Samareh 1990). Ideally, the geometry parametrization method must:

1. Be able to generate a large number of physically realistic shapes with as few design variables as possible.
2. Be robust, meaning that a random perturbation of the design variables should still provide a realistic blade.
3. Be able to import any existing geometries from CAD files in very little engineering time, few computational resources, and to an arbitrary accuracy specified by the designer.
4. Be generic to be applied to a large number of shape optimization problems and able to be integrated or coupled with any existing CAD system.
5. Provide design variables that can easily be handled by an engineer to define design variable bounds.
6. Provide an easy optimization problem by minimizing the skewness and improving the conditioning of the design space.

In this study, the geometry is parametrized using a simple yet very efficient and generic method using B-spline curves. The location of the B-spline control points are chosen such as to minimize the discrepancy between the B-spline definition of the blade geometry and the existing discrete target blade shape to be parametrised. This methodology is general and can be applied to any curve parametrization which can therefore be used to parametrize any shape in any design problem. The design variables can define a modification either with respect to the existing original shape or an absolute shape.

In the present application, the optimization software developed at CENAERO (MAX) is used to perform the optimization. This software allows performing derivative-free optimization with a reduced number of calls to the computational intensive simulation software. The method is based on the construction of an approximate model (also called metamodel or response surface) and the use of a genetic algorithm to find the optimum predicted by the approximate model (Pierret and Van den Braembussche 1998; Pierret et al. 2004; Pierret 2005).

This paper presents several applications of this optimization method. First, the performance of the method is demonstrated on algebraic test functions. Then, a parametric study is performed to investigate the design space and identify the noise that is usually present in optimization tasks involving finite volume or finite element analysis. Next, a real two-dimensional and existing turbine blade geometry is optimized using the present method. The performance of the genetic algorithm is compared to the performance of the coupled method involving the approximate model and the genetic algorithm.

This methodology has been developed and is demonstrated on the redesign of the full three-dimensional shape of the NASA rotor 67 geometry. Moreover, the geometry is optimized for several operating points simultaneously, large number of design variables, and using aerodynamic and structural mechanics analysis software.

2 The optimization strategy

2.1 Basic principle

The basic principle of the optimization algorithm developed in this research project is based on the use of genetic algorithms (GA) because they provide a very robust method satisfying many of the criteria mentioned above (Goldberg 1994). Moreover, constraint handling with GA is easily performed using a method proposed in (Deb 2000). The method proposes to use a tournament selection operator, where two solutions are compared at a time, and the following criteria are always enforced:

1. Any feasible solution is preferred to any infeasible solution.
2. Among two feasible solutions, the one having better objective function value is preferred.
3. Among two infeasible solutions, the one having smaller constraint violation is preferred.

One drawback of GAs is that they suffer a slow convergence because they use probabilistic recombination operators to control the step size and searching direction. As a consequence, for real industrial problems involving expensive function evaluations, the GA required CPU time is usually not practical even with nowadays computing power. Therefore, a lot of effort has been put in this research project to accelerate the optimization process by using approximate model and using robust and efficient genetic operators.

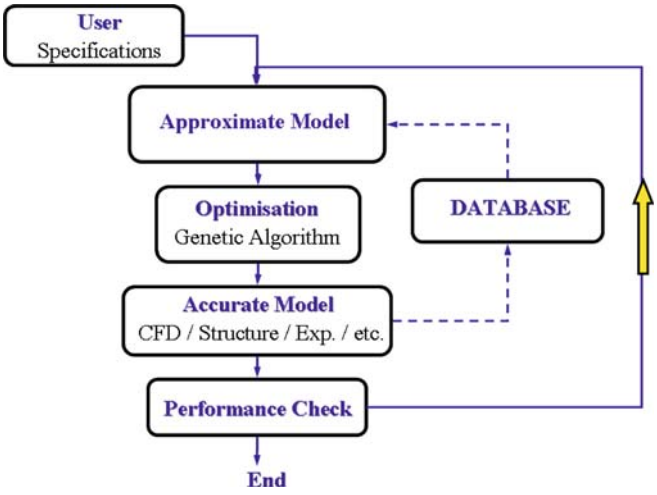

Fig. 1 Optimization strategy diagram

The blade design algorithm is represented in Fig. 1 and is organized as follows:

1. The first step consists in building a database using a design of experiments procedure (DOE). Numerous techniques exist: full factorial, fractional, central composite, D-optimal, Latin-hypercube, and random selection among others.
2. Second, an approximate model is built using the design of experiment points to construct an analytical relation between the design variables and the simulation responses.
3. Third, an optimization algorithm is used to find the optimum using the approximate model to evaluate the objective functions and constraints. One single approximate model is used to evaluate all the objectives and constraints.
4. Fourth, the accurate simulation is used to evaluate and verify the actual values of the objectives and constraints. This new simulation result is added to the database. The database is therefore always improved with new design points therefore leading to an improved approximate model.
5. Go to step 2 until the maximum number of optimization cycles specified by the user is not reached.

In this work, the design of experiments is very often performed using random selection of design points improved with techniques to ensure a maximum filling of the design space. This is a generic method because it allows generating a number of points independently on the number of design variables. DOE can very often be generated very rapidly by making use of massively parallel computers to evaluate the expensive objective functions. The software developed in this research is parallelized using MPI. In general, the number of design points generated in the DOE is equal to one to two times the number of design variables. At every optimisation cycle, a new approximate model is constructed using all the data points available in the database.

Several multidimensional and nonlinear interpolation techniques can be used to construct the approximate model. They are kriging (Chung and Alonso 2002), artificial neural network (Masters 1995), radial basis function network (Bishop 1995), or lazy learning (Bontempi et al. 2001) among others. Compared to simple polynomial interpolations, these techniques offer the advantage of decoupling the number of free parameters in the model with respect to the number of design parameters. In this research, the radial basis function interpolation technique is very often used mainly because of its robustness in providing an accurate approximate model. Moreover, it allows constructing a global approximate model which is valid for the entire design space. This is an important aspect for the application of the method to multiple objective optimization techniques based on the Pareto front concept.

2.2 Validation and performance

The scope of the numerical experiment in this section is to validate the capabilities of the design method to find the global objective function optimum of a multimodal function and to assess the convergence speed of the optimization algo-

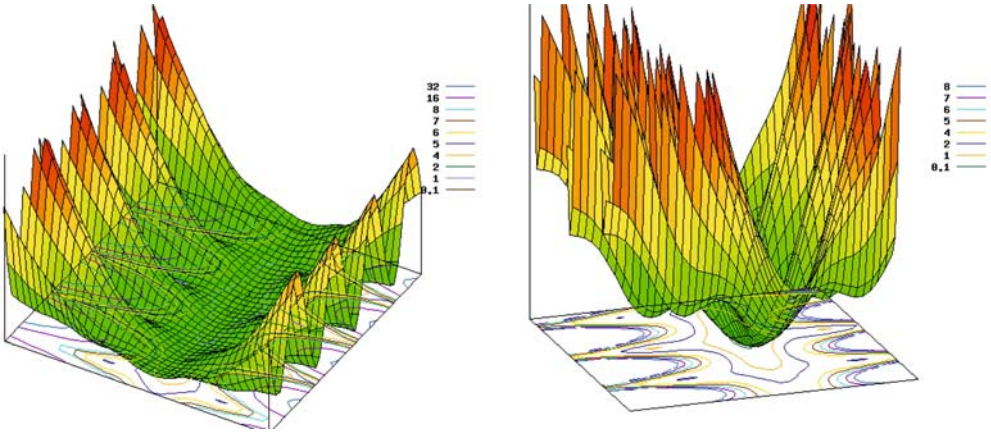

Fig. 2 Multi-modal function (*left*) and closer view on the local minima of the multimodal function (*right*)

rithm. This function with two design variables is represented in Fig. 2, and the exact mathematical definition is provided in (1). Figure 2 also provides a closer view on this test function to better visualize the local minima.

$$f = sin\Big(3.14159 * \big[1 + (x[0] - 1)/4\big]\Big) * sin\Big(3.14159 * \big[1 + (x[0] - 1)/4\big]\Big) + \big(1 + (x[n] - 1)/4 - 1\big)^2 + \sum_{i=0}^{i<n-1} \big[(x[i] - 1)/4\big]^2 * \Big(1 + 10 * \Big[sin\Big(3.14159 * \big[1 + (x[i+1] - 1)/4\big]\Big)\Big]^2\Big) \quad (1)$$

This optimization test case is run using the same type of test function but with four design variables. With four design variables, the square domain $[-10, 10] \times [-10, 10]$ contains 625 local minima.

This optimization task is first solved using the genetic algorithm alone with a population of 50 individuals. The convergence history shows that the global minimum is found with a precision of 10^{-6} after 1,000 function evaluations.

Finally, the most interesting results using the GA accelerated by the approximate model is presented. An initial database with 12 points is used and then only 100 optimization iterations are required to find the global minimum with an accuracy of 10^{-6} (Fig. 3). This benchmark demonstrates the convergence speed up by a factor of 10 using the GA coupled to the approximate model. It also shows that the second method is capable of finding the global optimum of such a multimodal function.

3 Rotor 67 redesign

This test case aims at demonstrating the advantage of using this design method in a real complex industrial application involving large simulation cost, large number of design parameters, and multiple operating points optimization problems.

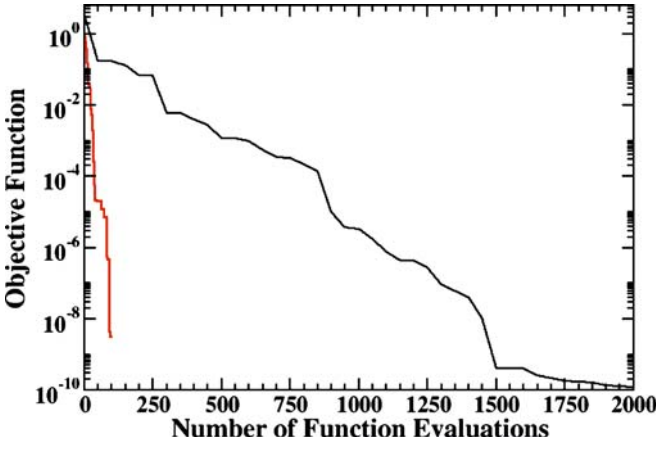

Fig. 3 Convergence history on the multimodal function

3.1 The test case

In the present study, the NASA rotor 67 geometry is used. This compressor is representative of fan blades. The rotational speed is 16,043 rpm, there are 22 blades and the design mass flow is 33.25 kg/s. The aim is to find the optimal geometry for three different operating conditions: one at choked mass flow, one at near efficiency peak, and one near the stall flow. The three points are analyzed at the same blade rotational speed which is the design speed.

In the context of this work, a computational code solving the Reynolds-averaged Navier–Stokes equations (RANS) is used to predict the aerodynamic performance of turbomachinery blades. The TRAF code which is developed by the University of Florence is used in this research (Arnone et al. 2003) and has been validated on several test cases among which the rotor 67 geometry (Arnone 1994).

A C-type mesh is used in this study. The mesh used for the computations contains 700,000 mesh points having 233 points along the C mesh lines, 53 from the blade walls to the midpitch and 57 in the spanwise direction. The code is capable of obtaining a converged solution in 1 h on a Xeon processor (3.06 GHz). The Baldwin–Lomax turbulence model is used.

The rotor 67 has been redesigned in several papers among with (Lian 2004; Oyama et al. 2002). In Oyama et al. (2002), the rotor is redesigned at one operating point using only aerodynamic computations. The blade is defined by 35 parameters. A genetic algorithm is used without the use of metamodels. A population of 64 individuals is used and the optimization is run for 100 reproduction cycles. This leads to 6,400 evaluations of the Navier–Stokes solution. The efficiency is improved by 1.78%.

First, the blade is redesigned using aerodynamic objectives and constraints only Section (3.2). Then the same geometry is optimized using aerodynamic and mechanical objectives and constraints Section (3.3).

3.2 The aerodynamic optimization

3.2.1 The objective function

Only aerodynamic objectives and aerodynamic constraints are imposed. The aerodynamic efficiency is maximized at

three operating points, while a lower limit is imposed on the pressure ratio at the three operating points. The mass flow computed by the TRAF code on the original geometry is 34.25 kg/s at choked mass flow. This mass flow is constrained between 34.15 and 34.25 kg/s during the optimization. Therefore, the objective function takes the following mathematical expression:

$$\begin{aligned} f(X) = {} & 50 * \eta_1 + 100 * \eta_2 + 50 * \eta_3 \\ & + 10^4 * max(1.46 - \pi_1, 0) \\ & + 10^4 * max(1.65 - \pi_2, 0) \\ & + 10^4 * max(1.73 - \pi_3, 0) \\ & + 100 * max(mf_1 - 34.25, 0) \\ & + 100 * max(34.15 - mf_1, 0) \end{aligned} \tag{2}$$

where:

1. η_1, η_2, and η_3 are the efficiencies at high, intermediate, and low mass flow (objectives).
2. π_1, π_2, and π_3 are the total pressure ratio at high, intermediate, and low mass flow (constraints).
3. mf_1 is the mass flow at the high-mass flow operating point (constraints).

3.2.2 The optimization results

The three-dimensional geometry is parametrized using five two-dimensional sections equally distributed from hub to tip. The two-dimensional sections are parametrized using B-Spline curves. Thirty-five design parameters are used in total defining modifications of the blade geometry with respect to the original blade shape. A first optimization run is performed using the GA alone. The genetic algorithm is run using a population of 60 individuals who are evaluated in parallel on 60 processors.

Figure 4 shows the optimization convergence history. With GA, a large gain is obtained during the first two reproduction cycles. Then, smaller amplitude gains are still obtained during the next reproduction cycles. However, this convergence history shows that a fully converged solution would probably require around 10,000 optimisation cycles.

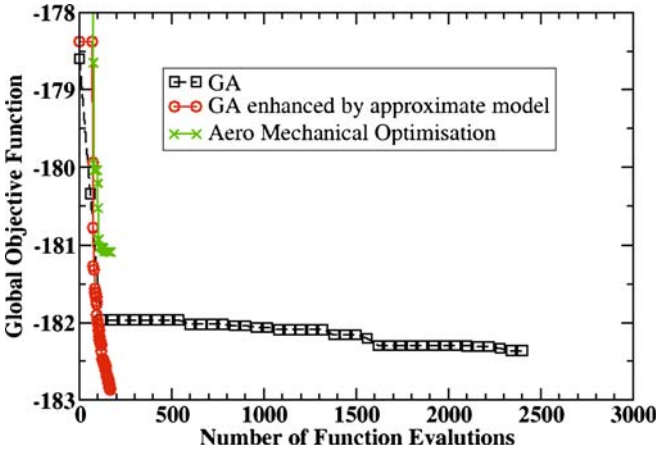

Fig. 4 Rotor 67—optimization convergence history

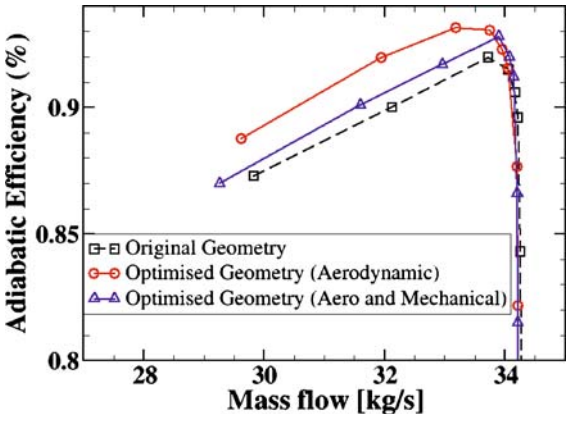

Fig. 5 Rotor 67—efficiency performance curve

The same optimization problem has been solved using the methodology based on the combined use of genetic algorithm and metamodel. This optimization process is first initialized by constructing a design of experiments based on 70 geometries run in parallel on a Linux cluster using 20 processors. Then, the optimization is run for 100 function evaluations. The convergence history obtained with the genetic algorithm and the genetic algorithm accelerated by the metamodel (Fig. 4) demonstrates that the second method is about 20 times faster than a classical genetic algorithm. Moreover, the optimum found by the second optimization algorithm is better and probably corresponds to the solution close to the fully converged solution. This fully converged solution could be found by the GA alone but would require too large computer resources to bring it to full convergence.

Figure 5 shows the compressor performance map at the design rotational speed for both the initial and optimized blade geometries. The adiabatic efficiency of this already highly optimized blade has been improved by more than 2% along the whole operating curve. The main reason for the efficiency improvement is probably the decrease of shock intensity mainly at midspan (Fig. 6).

Figure 7 shows the total pressure ratio curve for the original and optimized blade geometries. This pressure ratio is slightly larger along the whole curve.

Figure 8 highlights the geometry variations for three sections: at hub, at midspan, and close to the tip section. The tip section clearly shows a S-shape suction side. However, the tip section clearly has a negative thickness portion, while the midspan section has a very thin leading edge and the hub section has a too thin trailing edge. Although not realistic, the CFD analysis of a blade with negative thickness is possible because the mesh is generated around the blade without any intersection check between the suction and pressure sides. These small thicknesses of the optimized blade clearly demonstrate that mechanical objectives and constraints must be added to the optimization procedure to reject such blade geometries.

Figure 6 highlights the changes in the density contours on the suction side at the intermediate mass flow. In particular, the hub section shows a smaller amplitude of the shock, while

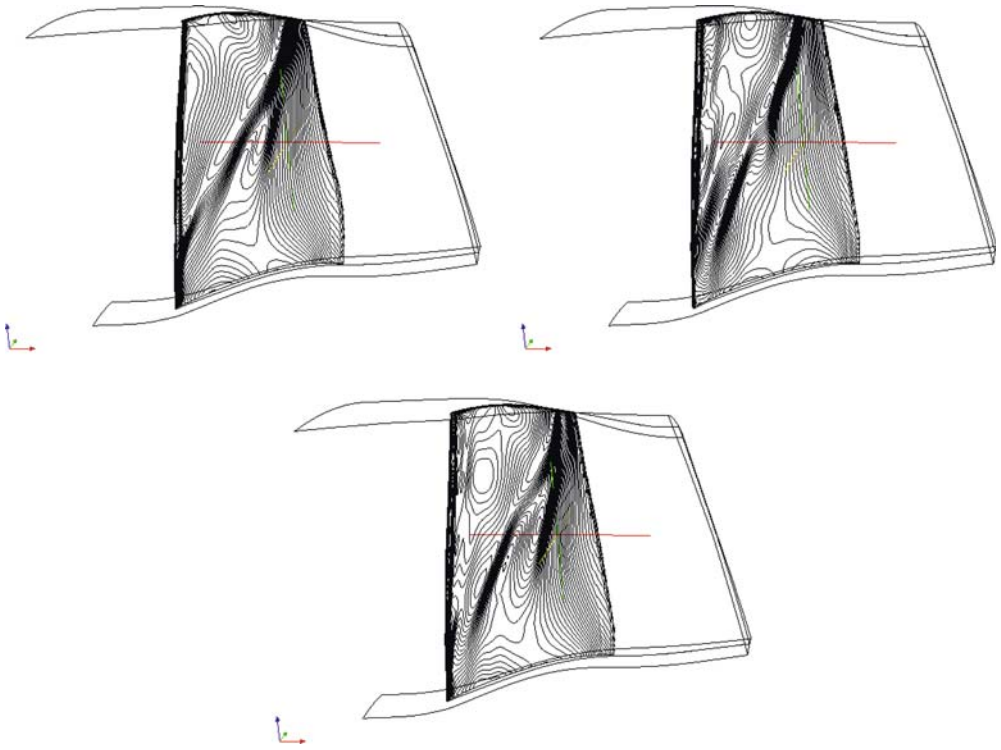

Fig. 6 Rotor 67—suction side density contours: initial geometry (*left*), aerodynamic optimization (*center*), and aeromechanical optimization (*right*) at the intermediate mass flow

the midspan section indicates that one of the two initial shocks along the suction side disappeared.

Figure 9 shows the isentropic Mach number distribution on three sections. The intensity of the shock wave on the tip section is clearly reduced. This is confirmed by the isentropic Mach number distribution along the tip pressure side. The midspan isentropic Mach number distribution is also smoother than on the original geometry and the shock intensity at midspan is reduced.

Figure 10 shows the outlet total pressure along the spanwise direction. It clearly shows large improvements in total pressure along the whole spanwise direction. Figure 11 presents the outlet flow angle along the spanwise direction. The outlet flow angle is decreased compared to the original geometry. As a consequence and in the context of a multistage machine, the next stator blade should be adapted to provide an optimum inlet flow angle.

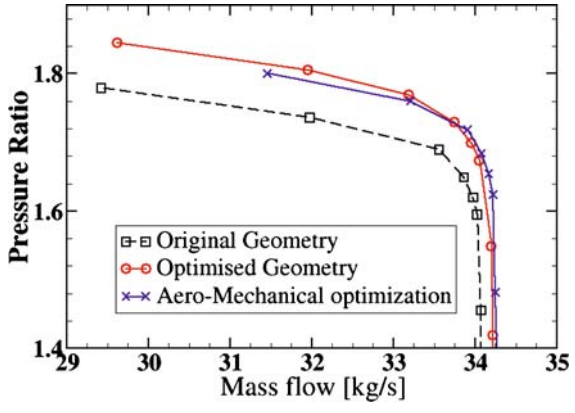

Fig. 7 Rotor 67—total pressure performance curve

3.3 The aeromechanical optimization

In this section, the same shape optimization problem is treated but a FEM structural mechanic code (SAMCEF) is used to compute the static stresses and dynamic vibration modes. These new responses are then included in the optimization process as constraints.

3.3.1 The aeromechanical simulation chain

The aeromechanical optimization process is summarized in Fig. 12. The simulation chain is composed of the following components:

- The shape parametrization module transforms the design variables into the detailed shape definition of the three-dimensional blade section.
- The FEM software computes the maximum von Mises stress and the blade vibration frequencies. The load case is imposed by the centrifugal forces due to the blade rotation. The FEM computational time is about 5 min and is therefore a lot cheaper than the computational time required by the CFD simulation (1 h).

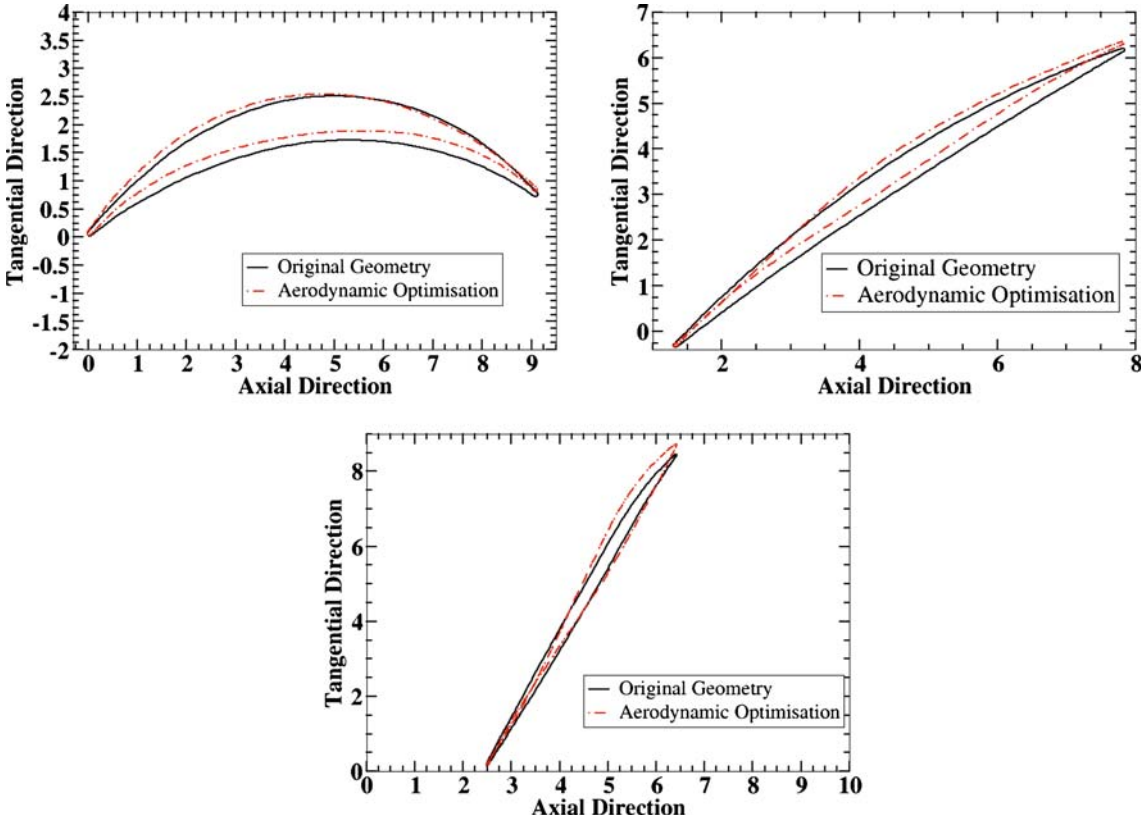

Fig. 8 Rotor 67—section geometry obtained with aerodynamic optimization—hub section (*top–left*), mid section (*top–right*), and tip section (*bottom*)

– The CFD software including the mesh generation, the flow solver, and the postprocessor extracts aerodynamic responses such as the aerodynamic efficiency, the pressure ratio, and the mass flow. Three CFD computations are performed for three different static pressure imposed at the domain outlet boundary.
– The parallel application manager, which is a MAX component, is capable of managing the simulation submission based on many criteria such as the number of available processors and number of available software licenses.
– The optimization based on the metamodel.
– The database containing the initial DOE results together with an incremental storage of the simulation responses computed by the simulation chain.

The Samcef finite element model used for the blade simulation consists of 20×20 nodes forming a volumic shell with varying thickness along the blade geometry. This mesh and FEM approach are probably not appropriate enough to provide an accurate prediction of the real eigen frequencies. An accurate prediction would require a volumic FEM approach together with the modelling of the blade root and disk. However, this model is adequate for the purpose of demonstrating the capabilities of the optimization approach presented in this study to handle a large number of constraints where the constraints are various forbidden ranges on the system responses. The centrifugal forces are imposed while the fluid pressure is not imposed on the FEM computation in this study. The FEM code is run to compute both the static and dynamic blade behaviors. The 20 first vibration frequencies are computed at 0 rpm, at the nominal rotational speed (16,043 rpm), and at 105% of the nominal rotational speed.

An imaginary material is used for this computation whose properties are taken identical to the values used for a fluid/structure interaction performed in (Doi and Alonso 2002). The Young's modules, Poisson's ratio, and metal density are chosen to be E=1.422e+11 Pa, $\nu = 0.3$, and $\rho =$ 4,539.5 kg/m^3, respectively, which looks reasonable when comparing the vibration frequencies of the original blade with the aerodynamic excitation frequencies.

The five first vibration frequencies at cruise speed on the original geometry are: 557, 1,307, 1,923, 2,760 and 3,111 Hz.

3.3.2 The objective function

The objective function contains the objectives and constraints already defined for the pure aerodynamic optimization. However, several mechanical constraints are added. The first one aims at limiting the maximum static stresses inside the blade metal. This is performed by imposing a maximum limit on the Von Mises stress to 4.8 MPa compared to a value of 4.75 MPa on the initial geometry.

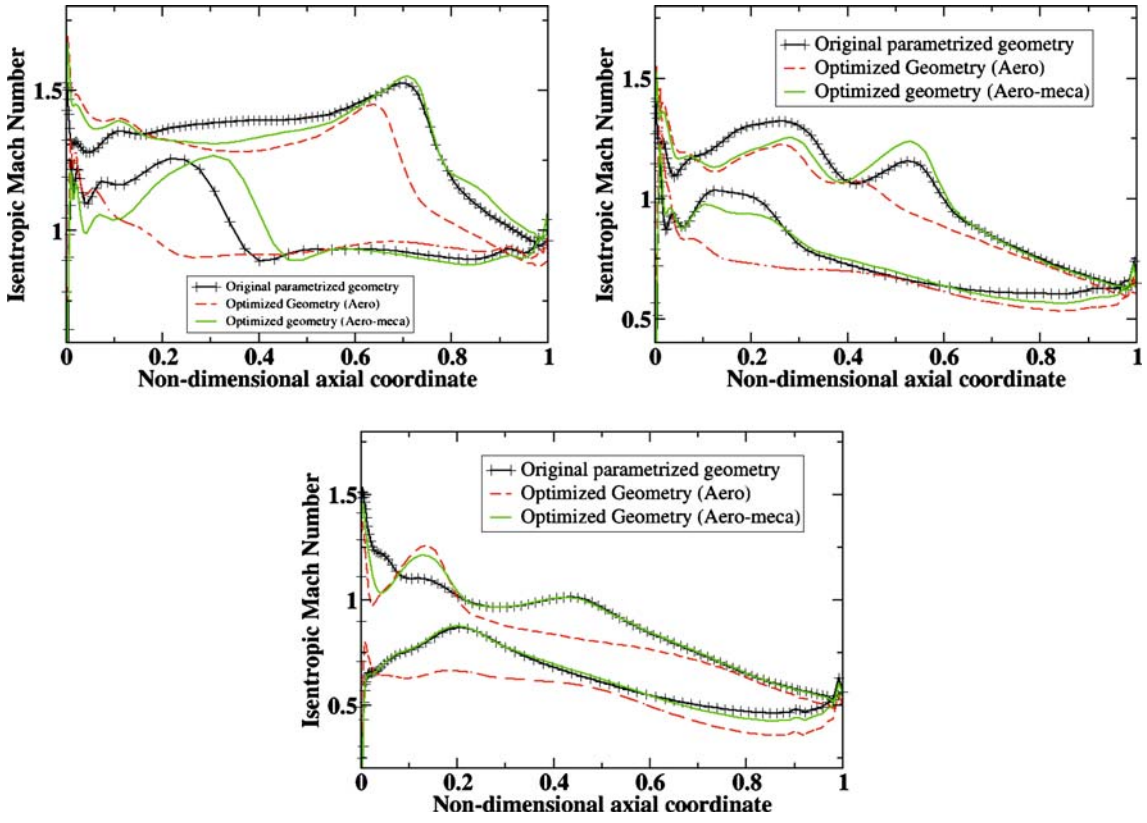

Fig. 9 Rotor 67—isentropic Mach number at the intermediate mass flow–tip section (*top–left*), mid section (*top–right*), and hub section (*bottom*)

The vibration frequencies are controlled at cruise speed by imposing several constraints on the first and second vibration frequencies. The rotational speed is 16,043 rpm or 267.4 Hz. This value is defined as N=267.4 Hz. In practice, the blade vibration frequencies should not be equal to 1, 2, 4, 8 N, etc. Moreover a margin of +/−5% is imposed with respect to these forbidden frequencies leading to the following forbidden ranges: 260–274, 521–548, 1,042–1,096, 1,564–1,644, and 2,085–2,192 Hz. Then the first and second blade vibration frequencies are not allowed to be inside these ranges.

3.3.3 The optimization results

The convergence history is represented in Fig. 4. The optimizer converges in 120 iterations. The objective function value decreases compared to the initial value but the level reached at the end of the optimization is higher than the one obtained with the pure aerodynamic optimization. This is normal due to the additional constraints imposed during the aeromechanical optimization.

The efficiency gain is represented in Fig. 5. The efficiency gain with the aeromechanical optimization is of 0.5% along

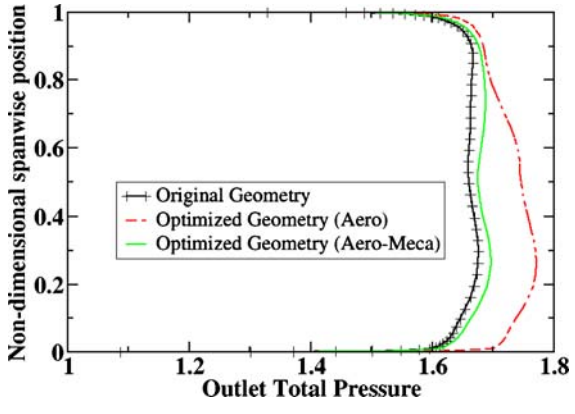

Fig. 10 Rotor 67—spanwise outlet total pressure (nondimensionalized by the inlet total pressure)

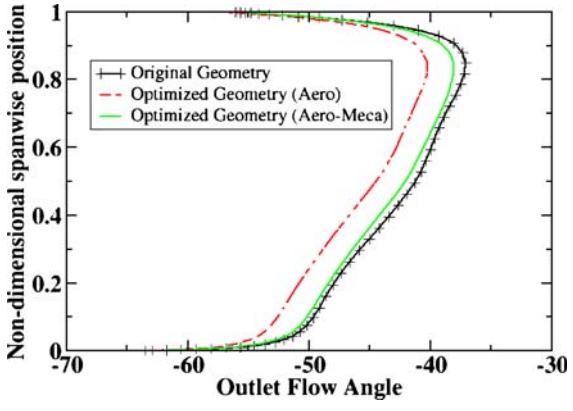

Fig. 11 Rotor 67—spanwise outlet blade-to-blade flow angle

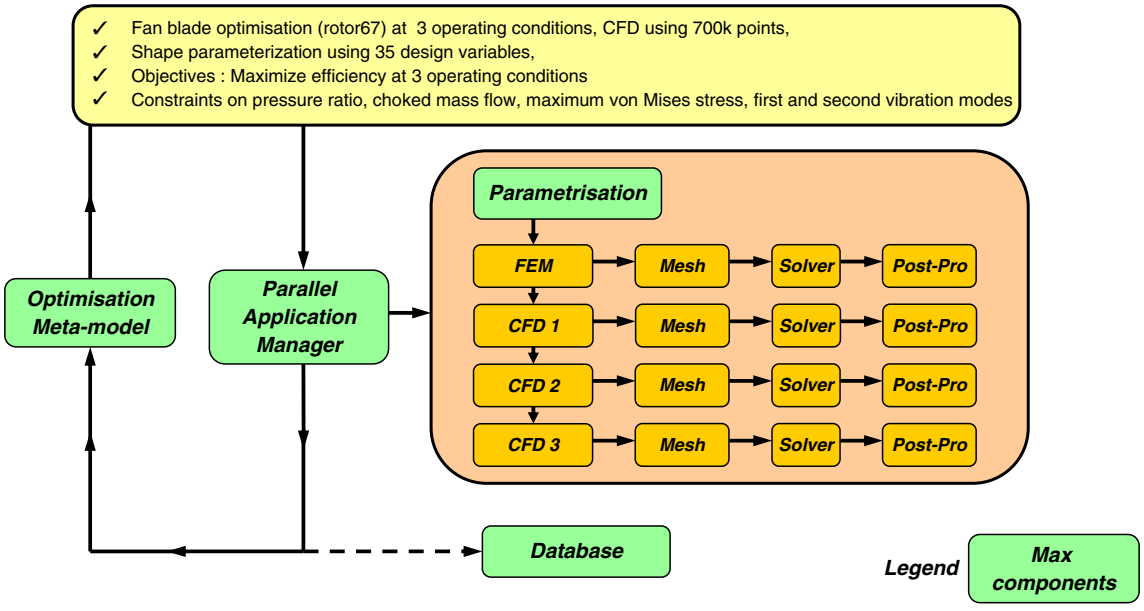

Fig. 12 Aeromechanical and multiple operating points optimization chain

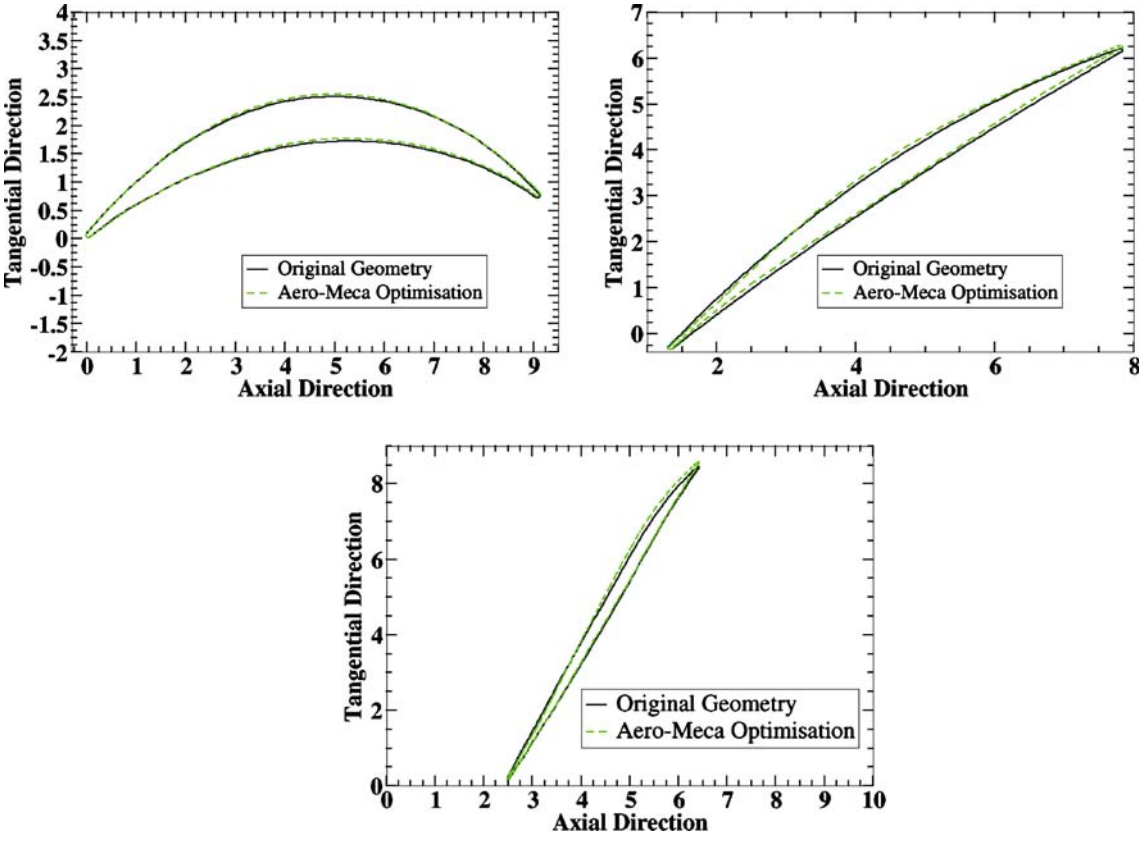

Fig. 13 Rotor 67—section geometry obtained with aeromechanical optimization—hub section (*top–left*), mid section (*top–right*), and tip section (*bottom*)

the whole operating range. This is smaller than the efficiency gain obtained for the aerodynamic optimization, but this is normal due to the additional constraints imposed in this second case.

The maximum von Mises stress of the optimized blade is 3.9 MPa, while the first two vibration frequencies are 599.6 and 1,360 Hz. These values are outside the forbidden ranges specified during the optimization.

Figure 13 shows that the blade thickness now looks much better than for the pure aerodynamic optimization. The blade thickness along the first part of the blade close to the leading edge is still small on the midspan and tip sections. This last point probably comes from the fact that only the centrifugal forces are imposed for the FEM mechanical computation and not the effect of the aerodynamic pressure field onto the three-dimensional blade shape. The next step of the current research will then be to impose the pressure field along the blade walls to further increase the simulation accuracy.

4 Conclusions

This paper demonstrates that optimization methods based on genetic algorithm accelerated by approximate models has many advantages compared to other design techniques: it provides efficient geometries in a very short time, can be run automatically, and mimics the intelligent behavior of the designer. It can manage uncomputable functions and does not require accessing the source code and, therefore, can easily be applied to any type of equations (Euler, Navier–Stokes, mechanics or acoustic among others).

The elapsed time required to perform the aeromechanical design of a three-dimensional blade is reduced to less than a week. This has to be compared to a time of more than 2 to 3 weeks required by an experienced designer team to "manually" design a three-dimensional blade including the aerodynamic and the mechanical objectives.

The optimization method has been largely validated on various test functions of which one test case is presented in this study. The genetic algorithm and DOE have been parallelized using the MPI library allowing for a rapid turn around time for the design of turbomachinery blades.

This paper presents the first results towards an effort to reduce the computational effort for real industrial optimization tasks involving multiple objectives and multiple disciplines (CFD, mechanics, thermal analysis, and acoustic).

A large step towards an automatic aeromechanical optimization chain has been performed. However, further developments are needed to further model the real process by including the pressure mapping of the fluid onto the three-dimensional blade.

Other improvements could also come from the use of larger number of design parameters. Moreover, by including directly the number of blades as a design parameter, its optimal value could also be found automatically by the optimization algorithm.

Acknowledgements The author wishes to thank the Wallon Region and the ERDF European funds which are funding this research project under contract n^o EP1A122030000102. The author is also very grateful to Prof. Arnone, Michele Marconcini and the Department of Energy Engineering "Sergio Stecco" of the University of Florence for making the TRAF code available for conducting this research and for providing user support.

References

Arnone A (1994) Viscous analysis of three-dimensional rotor flow using a multigrid method. J Turbomach 116:435–445

Arnone A, Marconcini M, Scotti Del Greco A (2003) Numerical investigation of three-dimensional clocking effects in a low pressure turbine. ASME 2003-GT-38414, ASME Turbo Expo Conference 2003, Altanta, Georgia, USA

Bishop CM (1995) Neural networks for pattern recognition. Oxford University Press, New York

Bontempi G, Bersini H, Birattari M (2001) The local paradigm for modeling and control: from neuro-fuzzy to lazy learning. Fuzzy Sets Syst 121:59–72

Chung HS, Alonso JJ (2002) Using gradients to construct cokriging approximation models for high-dimensional design optimization problems. AIAA 2002-0317—40^{th} AIAA Aerospace Sciences Meeting and Exhibit, January 14–17, 2002/Reno NV

Deb K (2000) An efficient constraint handling method for genetic algorithms. Comput Methods Appl Mech Eng 186:311–338

Doi H, Alonso JJ (2002) Fluid/Structure coupled aeroelastic computations for transonic flows in turbomachinery. ASME GT-2002-30313, ASME Turbo Expo Conference 2002, Amsterdam, The Netherlands

Goldberg DE (1994) Genetic algorithms. Addison–Wesley, MA

Lian Yongsheng (2004) Multi-objective optimization using coupled response surface model and evolutionary algorithm. AIAA paper 2004-4323, $10th$ AIAA/ISSMO Multidisciplinary Analysis and Optimization Conference, Albany, New York, USA

Masters T (1995) Practical Neural Network Recipes in C++. Wiley, New York

Oyama A, Liou MS, Obayashi S (2002) Transonic axial-flow blade shape optimization using evolutionary algorithm and three-dimensional Navier–Stokes Solver. AIAA paper 2002–5642

Pierret S (2005) Multi-objective optimization of three-dimensional turbomachinery blades. International Conference on Computational Methods for Coupled Problems in Science and Engineering, 25–28 May 2005, Santorini Island, Greece

Pierret S, Van den Braembussche RA (1998) Turbomachinery blade design using a navier-stokes solver and artificial neural network. ASME paper 98-GT-04, ASME Turbo Expo Conference 1998, Stockholm, Sweden

Pierret S, Ploumhans P, Gallez X, Caro S (2004) TurboFan noise reduction using optimization method coupled to aero-acoustic simulations. Design Optimization International Conference, ERCOFTAC 2004, March 31—April 2, Athens, Greece

Samareh JA (1990) A survey of shape parametrization techniques. CEAS/AIAA/ICASE/NASA Langley International Forum on Aeroelasticity and Structural Dynamics, June 22–25, 1990—Also NASA/CP-1999-209136